JOURNAL OF MAGNETIC RESONANCE **134,** 142–153 (1998)
ARTICLE NO. MN981520

The Effects of Cryoprotection on the Structure and Activity of p21 *ras:* Implications for Electron Spin-Echo Envelope Modulation Spectroscopy[1]

Christopher J. Halkides,* Christian T. Farrar,†,[2] and David J. Singel‡

**Department of Chemistry, University of North Carolina at Wilmington, Wilmington North Carolina 28403-3297; †Department of Chemistry, Harvard University, Cambridge, Massachusetts 02138; and ‡Department of Chemistry and Biochemistry, Montana State University, Bozeman, Montana 59715*

E-mail: halkidesc@uncwil.edu

Received November 14, 1997

Electron spin-echo envelope modulation (ESEEM) spectroscopy is widely used to investigate the active sites of biological molecules in frozen solutions. Various cryoprotection techniques, particularly the addition of co-solvents, are commonly employed in the preparation of such samples. In conjunction with ESEEM studies of Mn(II) guanosine nucleotide complexes of p21 *ras,* we have investigated the effects of cryoprotection on the spectroscopy, the structure, and the activity of this protein. Echo decay times, which typically govern ESEEM spectral resolution, were found to vary linearly with the concentration of glycerol or methyl α-D-glucopyranoside (MG), with both additives equally effective on a per-mole basis. The effect of glycerol and MG on the ESEEM amplitudes of various protein nuclei was studied in *ras* p21 · Mn(II) · 5′guanylylimido-diphosphate (p21 · Mn(II)-GMPPNP) complexes: these additives did not alter the distances of these nuclei from the Mn(II) ion. In particular, in p21 incorporating [^{2}H-3]Thr, the Mn(II)-[^{2}H-3]Thr35 distance was found to be unaffected by the concentration of cryoprotectant or the rate of freezing. The proximity of the cryoprotectants to the Mn(II) ion was probed by ^{2}H ESEEM in solutions made with d_5-glycerol and d_7-methyl α-D-glucopyranoside (d_7-MG). In p21 · Mn(II)GMPPNP, the large deuterium modulations from the d_5-glycerol exhibit saturation behavior with increasing d_5-glycerol concentration, implying that glycerol, a widely used cryoprotectant, replaces the aquo ligands of the Mn(II) ion. The interaction between the Mn(II) ion of p21 and MG, however, is less intimate: the deuterium ESEEM amplitudes are much smaller for samples prepared with d_7-MG than with d_5-glycerol. Several polyhydroxylic compounds were found to have essentially no effect on the ability of the guanosine 5′-triphosphate (GTP) hydrolysis activating protein, GAP334, to catalyze hydrolysis of p21 · guanosine 5′-triphosphate. This observation implies that the introduction of cryoprotectant does not significantly perturb the structure of p21 and gives insight into the mechanism of the GTPase reaction.

Key Words: ras; **cryoprotection**; **glycerol**; **ESEEM**; **spray-freezing.**

INTRODUCTION

A variety of techniques in structural biology and biochemistry employs frozen solutions to exploit the numerous advantages of low sample temperatures. In the realm of magnetic resonance spectroscopy, these advantages begin with increased sensitivity from larger Boltzmann factors at low temperatures. In addition, interactions that would be averaged out in solution, such as dipolar couplings, are retained in frozen solutions (*4*). In electron paramagnetic resonance (EPR) spectroscopy, the reduction in spin relaxation rates achieved at low temperatures is often crucial to the observation of paramagnetic species such as transition metal ions. Likewise, extremely low sample temperatures are typically required for the observation of electron spin echoes, which are central to the electron spin-echo envelope modulation (ESEEM) method, pioneered by Mims, Peisach, and their collaborators (*5, 6*). Our ongoing ESEEM studies of the structure of Mn(II) guanosine nucleotide complexes in the protein p21 *ras* are performed on frozen-solution samples at a temperature of 4.2 K (*1*).

When biological samples in aqueous solution are frozen, precautions must be taken to inhibit the segregation of the sample into a purified ice phase and a second phase that contains concentrated solutes (*7–9*); this segregation phenomenon can have several adverse effects on the sample. The shear associated with ice crystal formation can damage biological specimens (*10*). Proteins within the solute-rich phase can experience detrimental changes in ionic strength and pH (*7, 9*). An increase in local concentration of a paramagnetic species upon freezing can lead to a loss of resolution in EPR (*8*), electron-nuclear double resonance (ENDOR) (*11*), and ESEEM (*5*) spectra, presumably as a result of increased structural microheterogeneity and/or electron spin–spin interactions.

A primary technique employed to inhibit damage from freezing is the addition of cryoprotective co-solvents or solutes, typically polyalcohols or sugars (*12, 13*). Cryoprotectants retard the formation of the purified ice phase by lowering the

[1] This work was supported in part by National Institutes of Health under Grant 5R 37 GM20168 (to A. G. Redfield), C. J. H. was supported by NIH postdoctoral fellowship CA08872. C. T. F. was supported by NIH training Grant 5 T32 GM08313-04.

[2] Present address: Francis Bitter Magnet Laboratory, Massachusetts Institute of Technology, Cambridge, MA 02139.

1090-7807/98 $25.00

temperature of homogeneous nucleation, and thus facilitate the formation of a glassy phase in which the distribution of diffusible components, and thus the relevant interactions between components of the system, is maintained (*12, 14*). The addition of glycerol or sucrose to protein solutions has been found to stabilize the protein (*15*) and to protect against inactivation during cold-storage, freezing, thawing, or lyophilization (*16–18*). Cryoprotectants play a crucial role in cryoenzymology (*19, 20*) and are widely employed in biological microscopy, diffractometry, and spectroscopy (*21–23*). Glycerol is routinely added to protein solutions to improve spectral characteristics in ESEEM (*5*), ENDOR (*24, 25*), and EPR spectroscopy (*26*).

A second method to limit ice formation during the freezing process is to increase the rate of cooling (*7, 27*). Cooling rates may be increased by using cryogenic liquids with low melting and high boiling points (*7*) or by replacing the cryogen altogether with a rapidly spinning metal block (*28*), and by increasing the surface area of the sample by dispersing it into small ($\sim 10^{-3}$ μL) particles. These tactics are combined in spray-freezing techniques, which have been found to decrease protein aggregation markedly as compared to rapid cooling of undispersed, microliter-volume samples (*29*). Spray-freezing has also been used in conjunction with cryoprotective additives (*27*). Arguably the most important application of the spray-freezing technique is the rapid quenching of dynamic processes, which enables the study of reactive species (*28, 30–32*).

Our interest in p21 *ras* is broadly motivated by the important functional properties of this protein: its absolute requirement in signal transduction for cellular growth or differentiation, and its occurrence in point-mutant forms in about 30% of all human tumors (*33*). The critical role that protein–protein interactions play in key aspects of its function—including signal transduction, nucleotide exchange, and GTP hydrolysis (*34*)—provides a further impetus to our ESEEM studies: ESEEM is well-established as a local structural probe, applicable to high molecular weight, complex biological molecules in frozen solutions (*5*) and is thus ideally suited for probing structural transformations that accompany the interaction of p21 with its auxiliary proteins. An important component of this ESEEM approach to structural biology is to confirm that the cryoprotective additives introduced and freezing methods utilized do not significantly perturb the protein. Such checks are routine in the area of cryoenzymology (*19, 20*), but are less common in spectroscopy (*6*).

The issues raised in our ESEEM and EPR studies of p21 (*1, 35*) heighten the importance of careful scrutiny of the freezing technique. ESEEM measurements give results that closely match the X-ray structures in the phosphate-binding region of the protein, but differ in a region that undergoes a conformational change of pivotal importance to the signaling process. Specifically, the distance between the divalent metal and various nuclei in Thr35 in the Switch I region of the protein was found by ESEEM (*1, 35*) and EPR (*2, 36*) to be significantly larger than in the crystal structures. X-ray structures of p21 with a GTP analog, 5′-guanylylimido diphosphate (GMPPNP), show the Thr35 hydroxyl group to be coordinated to the divalent metal ion. This ligation has been suggested to be the driving force in the switch-actuating conformational change (*3, 34, 37*)—a notion difficult to reconcile with the ESEEM (*1*) and EPR results (*36*). Since the presence of glycerol additives or the freezing methodology could conceivably affect the protein structure, it is especially important to rule out the possibility that this structural distinction is an artifact of sample preparation methods.

Accordingly, we have experimentally surveyed various freezing methods and cryoprotective additives and have evaluated their effects from spectroscopic, structural, and functional perspectives. Variation of the cryoprotective compound, its concentration, or the rate of sample cooling is found to produce large changes in echo decay rates and thus in ESEEM spectral resolution. In addition, we find a surprisingly intimate interaction between the active site Mn(II) ion and the cryoprotectant glycerol, which is observed to replace metal-coordinated aquo ligands. This interaction, which clearly raises the *possibility* of cryoprotectant-induced structural distortion, is not manifest when the bulkier, closed-chain cryoprotectant, MG, is used. Notwithstanding these important effects, we find that the local protein structure, as directly gauged by the ESEEM-determined Mn(II)-Thr35 distance, is not significantly perturbed by cryoprotectant techniques. Moreover, the ability of p21 to hydrolyze guanosine-5′triphosphate (GTP) in the presence of the truncated GTPase-activating protein (GAP334) is likewise unaffected by the presence of cryoprotectants in solution. These results specifically establish the structural and functional innocence of the cryoprotective methods that are employed in ESEEM studies of p21. They give insight into the comparative utility of different freezing methods, and more generally, delineate the types of control experiments that can be performed to confirm the innocence of freezing methods used in low-temperature ESEEM spectroscopy.

RESULTS

Phase memory time as functions of cooling conditions. In two-pulse ESEEM experiments, the electron spins are subjected to a $\pi/2$ pulse, a delay of length τ, and a π refocusing pulse. The echo is observed at a time τ after the second pulse. The value of τ is increased in small increments, and the amplitude of the echo is plotted as a function of τ. Such ESEEM patterns typically show nuclear modulation effects superimposed on a decaying echo signal. The rate of this decay, gauged by the phase memory time (T_m), determines the ESEEM spectral linewidths (when T_m^{-1} is appreciably greater than the inherent ESEEM spectral linewidths) and resolution. Figure 1 shows a sampling of electron spin-echo envelopes (amplitude of the echo versus τ) for p21 in various frozen solutions, with clear variations in T_m.

All of the samples studied exhibited decay profiles that are fit by single exponential-decay functions. The exponential-decay constants obtained by analysis of the data are listed as

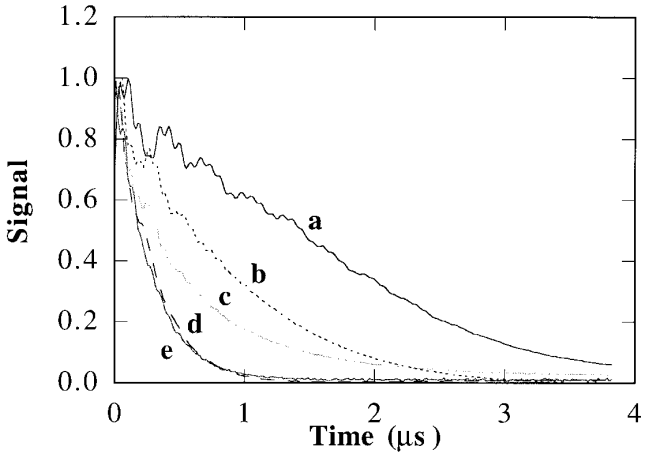

FIG. 1. Time-domain ESEEM patterns of p21 · Mn(II)GMPPNP as a function of cooling conditions. (A) Sample was plunge-frozen in liquid N_2 in the presence of 50% glycerol. (B) Sample was plunge-frozen in liquid N_2 without glycerol. (C) Sample was spray-frozen in the absence of glycerol. (D) Sample was plunge-frozen in isopentane in the absence of glycerol. (E) Sample was plunge-frozen in ethane in the absence of glycerol.

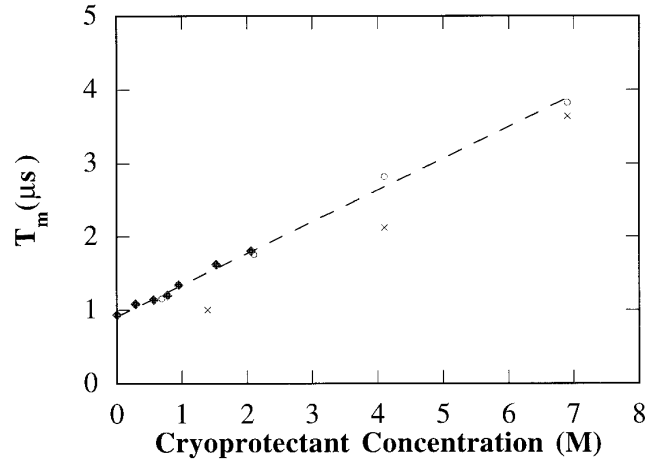

FIG. 2. Relaxation time (T_m) as a function of concentration and type of cryoprotectant. Relaxation times appear to increase linearly with increases in concentration of cryoprotectant. The solid diamonds represent different concentrations of MG; the open circles represent different concentrations of d_5-glycerol; the crosses represent different concentrations of unlabeled glycerol.

the experimental T_m values in Table 1. The dependence of T_m on cryoprotectant concentration is of particular interest, inasmuch as this relation discloses the cost—in degradation of ESEEM spectral resolution—of curbing our use of exogenous cryoprotectants. Relevant data from Table 1 are plotted in Fig. 2, and illustrate that, in this system, T_m increases in an approximately linear fashion with the concentration of either glycerol or MG. Moreover, these two cryoprotectants give roughly equal protection at equal molar concentration. For example, the T_m values obtained with 15% glycerol and 40% MG solutions, both of which are ~2 M in cryoprotectant, are essentially the same. The data in Fig. 2 also show that deuteration of the glycerol leads to a small increase in T_m as compared to protioglycerol. This type of behavior is known to occur when nuclear spin flip-flops contribute significantly to the local-field fluctuations. Notably, this isotope effect is not evidenced upon deuteration of the MG (*vide infra*).

TABLE 1
Electron-Spin Phase-Memory Time (T_m) as a Function of Freezing Conditions

Cryoprotectant	Cryogen	Method of freezing	T_m (μs)[a]
50% d_5-glycerol	N_2	Plunge	3.8 ± 0.2
30% d_5-glycerol	N_2	Plunge	2.8 ± 0.1
15% d_5-glycerol	N_2	Plunge	1.77 ± 0.04
5% d_5-glycerol	N_2	Plunge	1.16 ± 0.01
50% glycerol	N_2	Plunge	3.6 ± 0.1
30% glycerol	N_2	Plunge	2.12 ± 0.05[b]
10% glycerol	N_2	Plunge	1.01 ± 0.02
0%	N_2	Plunge	0.94 ± 0.01
0%	Ethane	Plunge	0.27 ± 0.01
40% d_7-MG	N_2	Plunge	1.81 ± 0.03
30% d_7-MG	N_2	Plunge	1.63 ± 0.05
20% d_7-MG	N_2	Plunge	1.35 ± 0.02
15% d_7-MG	N_2	Plunge	1.21 ± 0.01
10% d_7-MG	N_2	Plunge	1.14 ± 0.02
15% MG	N_2	Plunge	1.21 ± 0.02
15% MG	Isopentane	Plunge	1.09 ± 0.01
5% glycerol	Isopentane	Plunge	1.03 ± 0.01
0%	Isopentane	Plunge	0.27 ± 0.02[c]
5% MG	Isopentane	Spray-freeze	0.90 ± 0.01[c]
1.5% glycerol	Isopentane	Spray-freeze	0.68 ± 0.01
0%	Isopentane	Spray-freeze	0.49 ± 0.01

[a] The uncertainty represents the error in the fit.
[b] Average of three determinations.
[c] Average of two determinations.

To test the idea that plunge-freezing into an isopentane slush might largely reduce the need for cryoprotective additives, we measured T_m values of samples, thus frozen, with cryoprotectant concentrations of ~0.7 M (15% MG, 5% glycerol). We found that these samples behaved essentially the same as analogous samples frozen in liquid N_2: freezing in isopentane produced no significant benefit. In the complete absence of cryoprotective additives, plunge-freezing in isopentane slush or in liquid ethane actually appeared to yield poorer results (T_m 0.3 μs) than plunge-freezing in liquid nitrogen (T_m 0.9 μs). We similarly probed the comparative utility of spray-freezing with samples containing only ~0.3 M cryoprotectant to plunge-freezing in isopentane or liquid nitrogen in the presence of 0.5–0.7 M of cryoprotectant (5% glycerol or 10–15% MG). The spray-frozen sample had a slightly shorter decay time. Spray-freezing in the absence of cryoprotectant gave a result that was poor (T_m 0.5 μs), albeit slightly better than plunge-freezing cryoprotectant-free samples in isopentane or ethane.

In Fig. 3, we show two-pulse ESEEM spectra of [^{2}H-3]Thr/[^{13}C-4]Asx-labeled p21 · Mn(II)GMPPNP as a function of glycerol addition (0, 10%, and 50% glycerol). The peak at 2.1 MHz is ^{2}H from Thr35; the peak at 3.5 MHz is ^{13}C from

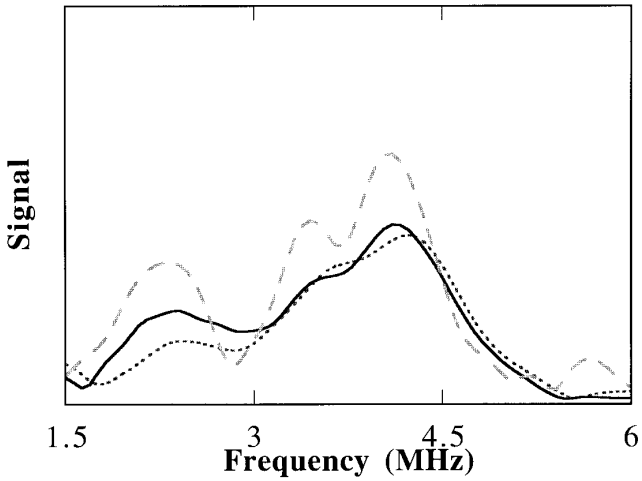

FIG. 3. Two-pulse ESEEM spectra of p21 · Mn(II)GMPPNP labeled with [^{2}H-3]Thr and [^{13}C-4]Asx in the presence of varying concentrations of glycerol. The dotted curve is in the presence of 0% glycerol, the solid curve is in the presence of 10% glycerol, and the dashed curve is in the presence of 50% glycerol. The field strengths of the three spectra were 3425, 3349, and 3272 G, respectively, for the spectra at 0%, 10%, and 50% glycerol. The EPR frequencies were 9.802, 10.042, and 9.858 GHz. The effect of increasing values of T_m with increasing concentrations of glycerol is evident as greater resolution between carbon and phosphorus and as greater overall signal-to-noise. The deuterium signal arises from Thr 35 and its amplitude yields a Mn(II)-^{2}H distance of 4.9 ± 0.2 Å, in all three cases.

Asp57; and the peak at 4.0 MHz is ^{31}P from GMPPNP (*1*). The effect of small T_m values on the ESEEM spectral resolution is clearly illustrated by these spectra: the absence of glycerol leads to the almost complete loss of resolution between carbon and phosphorus peaks.

The spectra in Fig. 3 also give important information regarding the impact of cryoprotectants on the p21 structure. The relative intensities of the ^{2}H, ^{13}C, and ^{31}P peaks are nearly identical in each of the spectra. Evidently, in stark contrast to the behavior of T_m, the hyperfine couplings of these nuclei are not sensitive to the freezing methodology. Detailed simulations of the [^{2}H-3]Thr peak in the presence of 0%, 10%, and 50% glycerol yield Mn(II)-[^{2}H-3]Thr35 distances that are identical within experimental error (namely 4.9 ± 0.2 Å) in the three samples. Figure 4 shows the spectra of analogous samples which were alternatively plunge-frozen in the presence of 15% MG or spray-frozen in the presence of 5% MG; both samples also yield a Mn(II)-[^{2}H-3]Thr35 distance of 4.9 ± 0.2 Å.

Deuteration of cryoprotectants. The addition of a cryoprotectant to an aqueous solution can be viewed, in effect, as a substitution of cryoprotectant molecules for various water molecules in the solvent. The active site of p21 is readily accessible to the solvent; the divalent cation in the active site has several aquo ligands. We were interested, therefore, to determine whether the cryoprotectant could replace not only water molecules in the bulk solution, but also those located in the active site of p21. The presence of cryoprotectant near the active site would be detected in a system containing a deuterium labeled cryoprotectant by a ^{2}H ESEEM signal. The amplitude of the ^{2}H ESEEM signal, as in the case of isotopically labeled protein, depends on the proximity of cryoprotectant molecules to the Mn(II) ion. Figure 5 depicts a series of ESEEM patterns for samples of p21 · Mn(II)GMPPNP in the presence of increasing amounts of d_5-glycerol (deuterated at the carbon positions). The low-frequency oscillations that increase in amplitude with increasing glycerol concentration arise from deuterium. Figure 6 shows a similar series for d_7-MG; the deuterium modulations are not nearly as strong in this series as in Fig. 5. The amplitude of the ESEEM peak at the ^{2}H Zeeman frequency, as a function of concentration of each cryoprotectant, is plotted in Fig. 7.

Two points are clearly illustrated in Figs. 5–7. First, at equal molarity, d_5-glycerol produces a much more intense 2H ESEEM signal than does d_7-MG, even though the two cryoprotectants have nearly identical effects on T_m (Table 1). Second, the ^{2}H ESEEM clearly exhibits a saturation effect with increasing cryoprotectant concentration. The solid lines in Fig. 7 represent binding-site saturation curves (Eq. [1]), generated with the least-squares best-fit dissociation constants: 0.8 ± 0.1 M (6% v/v) for glycerol, and 0.04 ± 0.4 M (0.8 % w/v) for MG. The dissociation constant for glycerol is better determined than the dissociation constant for MG. The asymptomatic amplitude of the deuterium modulations (24.7 for glycerol and 5.5 for MG) can be further analyzed to gain some insight into the location of the bound cryoprotectant. This estimation is facilitated by the stark distance-dependence (inverse sixth power) of ESEEM amplitudes, which thus tend to derive predominantly from the closest nuclei (*1*). By employing the

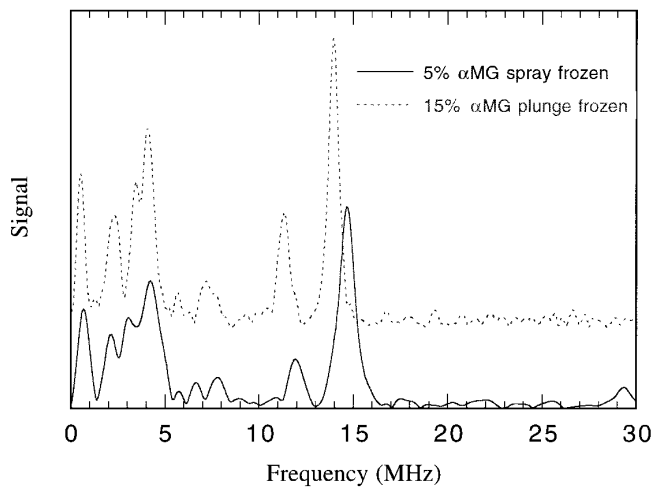

FIG. 4. Two-pulse ESEEM spectra of p21 · Mn(II)GMPPNP labeled with [^{2}H-3]Thr and [^{13}C-4]Asx spray-frozen in the presence of 5% MG (solid line) or plunge-frozen in the presence of 15% MG (dashed line). For the spray-frozen sample, peaks are apparent at 2.02 MHz (^{2}H), 3.06 MHz (^{13}C), 4.23 MHz (^{31}P), 11.92 MHz (^{31}P combination), and 14.65 MHz (^{1}H). The EPR frequency was 9.9375 GHz, and the field strength was 3441 G. For the plunge-frozen sample the EPR frequency was 9.858 GHz and the field strength was 3286 G. The deuterium signal arises from Thr 35 and its amplitude yields a Mn(II)-^{2}H distance of 4.9 ± 0.2 Å.

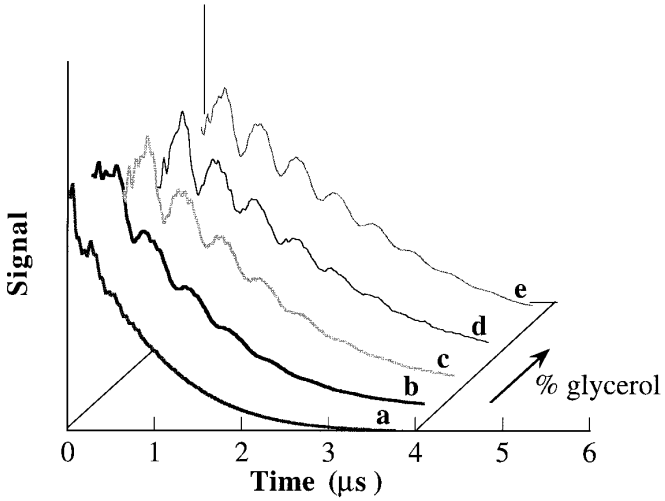

FIG. 5. Time-domain ESEEM signals of p21 · Mn(II)GMPPNP as a function of d_5-glycerol concentration by volume. The large, low-frequency oscillations arise from deuterium. Successive curves (A)–(E) show 0%, 5%, 15%, 30%, and 50% d_5-glycerol, respectively.

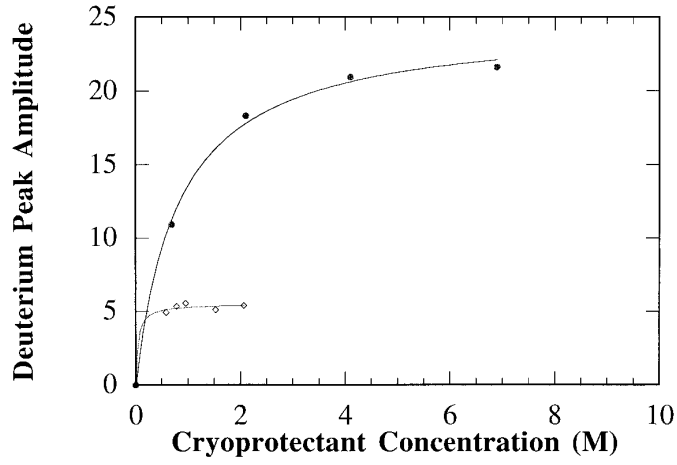

FIG. 7. The deuterium peak amplitude plotted as a function of concentration of deuterated cryoprotectant. Solid circles represent d_5-glycerol and open diamonds represent d_7-MG. The data for d_5-glycerol and d_7-MG were fit to a saturation curve as described in the Experimental section and dissociation constants of 0.8 ± 0.1 M and 0.04 ± 0.04 M were obtained for glycerol and MG, respectively.

single nucleus and equivalent nuclei approximations (*1*), we obtain lower and upper bound estimates of the distance of the deuterium atom(s) that are, by hypothesis, singularly close to the Mn(II) ion. For glycerol, these bounds embrace the range 3.1–4.1 Å. This result strongly suggests the coordination of a glycerol molecule to Mn(II) in place of aquo ligands. In contrast, the single-nucleus and the equivalent nuclei approximations for d_7-MG yield a distance range of 3.9–5.1 Å, incompatible with direct coordination.

GTPase assays. The rate of GTP hydrolysis catalyzed by p21 is greatly stimulated by the auxiliary protein GAP. The active region of GAP is located in the C-terminal 334 amino acid residues (*38*). The stimulation of the GTPase activity of p21 by a GAP protein truncated to this domain, namely GAP334, is shown in Table 2 as a function of sucrose or MG concentration, in aqueous solution. When 1 mM $MnCl_2$ replaces 1 mM $MgCl_2$, the GTPase rate is stimulated 3-fold (Table 2). Table 3 shows the GAP334-stimulated GTPase rate as a function of glycerol concentration. The data show that glycerol, sucrose, MG, or $MnCl_2$ have only modest effects on the rate of GTP hydrolysis.

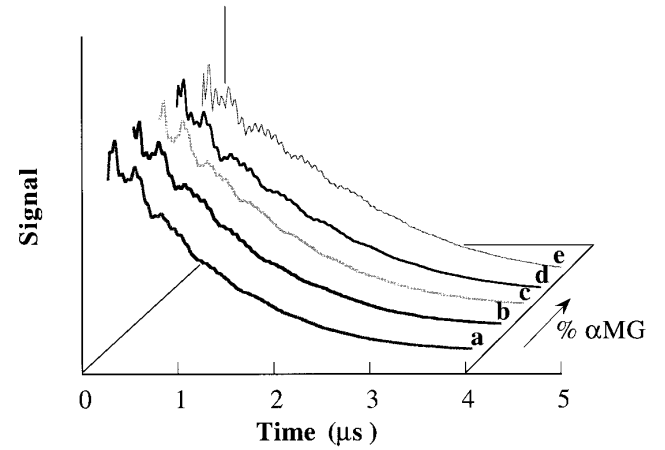

FIG. 6. Time domain ESEEM patterns of p21 · Mn(II)GMPPNP as a function of d_7-MG concentration by weight-percentage. The size of the deuterium oscillations is much smaller than in Fig. 4. Successive curves (A)–(E) show 10%, 15%, 20%, 30%, and 40% MG.

DISCUSSION

Echo decay times. We surveyed a variety of cryoprotective methods in an effort aimed at simultaneously optimizing phase-memory times to increase ESEEM spectral resolution, while minimizing the concentration of cryoprotective additives to reduce the risk of detrimental effects on protein structure and function. The variation of T_m with molar concentration of the additives glycerol and MG, shown in Fig. 2, is *linear* over the range 0–7 M. Accordingly, the co-solvent composition can be adjusted, *ad libitum,* to achieve the optimal compromise between resolution and additive concentration.

T_m is characteristic of the rate of fluctuations of local magnetic fields which arise from electron–electron or electron–nuclear interactions (*5*). The typical relation between T_m and the concentration of paramagnetic centers, C, can be expressed as $T_m^{-1} = \alpha + \beta C$, in which the constant α subsumes concentration independent effects such as nuclear spin diffusion, and β reflects the electron spin–spin effects that vary linearly with concentration (*39*). The concentration, C, must be understood as the local concentration of the paramagnetic center. If there were a separation of a pure ice phase during the freezing of the solution, then the Mn(II)-protein concentration in the remaining solution, that is, the local Mn(II)-protein concentration,

TABLE 2
The Effect of Sucrose, MG, or Mn(II) on the GAP334-Stimulated GTPase Rate of p21

Weight %	Relative GTPase rate (Sucrose)	Relative GTPase rate (MG)
0	1	1
5	0.86	0.61
10	0.75	1.51
15	0.72	0.78
0	3.0 (1 mM $MnCl_2$)	

would be increased by the freezing process and T_m would decrease (*5*). Within this framework, the variation of T_m with the concentration of cryoprotectant in the the solution demonstrates that the cooling rate and/or cryoprotectant concentrations employed were not sufficient to suppress ice formation totally. This result accords with the work of MacKenzie (*12*), who found that moderately fast freezing could not prevent ice nucleation at low concentrations of cryoprotectants but was required to prevent ice formation in solutions with moderate cryoprotectant concentrations.

We have found glycerol and MG are essentially identical, on a per mole basis, in increasing T_m, even though these additives interact with the protein in observably different ways (vide infra). This contrast reinforces the view that these additives exert cryoprotective effects by affecting properties of the bulk aqueous solvent, rather than the solvation of the protein. MacKenzie has observed that the additive-induced depression of the freezing point of water and its temperature of homogenous nucleation are linearly correlated (*12*). The former property, of course, depends only on the concentration of the additive, thus so also must the latter. Accordingly, the notion that cryoprotectants facilitate the formation of a glassy phase by lowering the temperature of homogenous nucleation is entirely in accord with our results.

In plunge-frozen samples, the properties of the cooling bath, that is, the nature of the cryogen, determine the cooling rate. We expected ethane and isopentane to provide more rapid cooling than liquid nitrogen and thus to enhance T_m (*7, 31*). We found, however, that nitrogen generally gave slightly better T_m values. Inasmuch as these observations are limited and no direct measurement of the cooling rate was undertaken (*7*), these data are more tentative. Nevertheless, they are in accord with results from cryocrystallography (*40*). The cooling rate can be dramatically increased through spray-freezing (*31, 32*), and we anticipated that spray-freezing might alleviate or possibly eliminate the need for cryoprotective additives altogether. We found, however, that samples spray-frozen in the complete absence of such additives exhibit unacceptably small phase-memory times. Our results are similar to those found for spray-frozen $CuCl_2$ and $MnCl_2$ solutions in EPR linewidth studies (*8, 41*). Likewise, solid-state ^1H or ^{13}C NMR studies of frozen glycine showed that spray-freezing did not markedly change the T_1 or the $T_{1\rho}$ values relative to slowly frozen samples (*42*). Some of these results may reflect the formation of a pure ice phase that can form during the removal of the cryogen (*8*). Spray freezing may allow one to reduce the concentration of cryoprotectant necessary to achieve the desired degree of vitrification (*27*); therefore, the combination of spray freezing and cryoprotection may be beneficial in cases where high concentrations of cryoprotectant are undesirable (*13*).

Deuteration of cryoprotectants. The large modulation amplitudes evidenced in Fig. 5 from deuterium labels in the samples of p21 · Mn(II)GMPPNP prepared in d_5-glycerol are striking, particularly as compared to the relatively small deuterium modulations from the d_7-MG samples exhibited in Fig. 6. At 2 M concentration of the cryoprotective additives, for example, the modulations in d_5-glycerol are about 4 times as large as in the d_7-MG, while the ratio of the number of deuterium atoms in the two compounds is 0.7. This disparity indicates that the additives are not simply dispersed in the bulk solvent—in which case the modulation depths would be nearly equal—but that each of the two additives interacts with the protein in some specific, but distinct manner. The disparate behavior of the deuterium ESEEM signals of these cryoprotectants extends to their concentration dependence: if these signals originated from bulk solvent molecules, their amplitude would show a *linear* increase with increasing concentration (*43*). As illustrated in Fig. 7, however, both systems show saturation behavior. The dissociation constants are 0.8 M for glycerol and 0.04 M for MG; the ratio of the limiting modulation amplitudes (glycerol vs MG) is ~4.5. These data indicate that the MG molecule that gives rise to the ESEEM interacts more avidly with p21 than does the corresponding glycerol molecule, but maintains a greater distance from the active site Mn(II) ion.

Detailed analysis of the deuterium modulation amplitudes, according to the *single nucleus* and *equivalent nuclei approximations*, is consistent with a single nucleus at 3.1 Å or with five equivalent nuclei at 4.1 Å from the Mn(II) ion. These values represent the lower and upper bounds, respectively, for distances from Mn(II) to deuterium atoms on the closest,

TABLE 3
The Effect of Glycerol on the GAP334-Stimulated GTPase Rate of p21

Volume % glycerol	Relative GTPase rate	Viscosity[a]
0	1.00	0.89
5	0.91	
10	1.09	1.06
15	0.74	
20	1.00	1.54
25	1.09	
30	0.66	2.12
40	0.75	3.18
50	0.69	5.2

[a] R. K. Scopes, "Protein Purification," Springer-Verlag, New York (1987).

labeled molecule, which is assumed [3] to dominate the ESEEM response. These distances are quite reasonable for an alcohol coordinated to a transition metal (*44*). The chelation of divalent metals, including Mn(II), by a hydroxyl group α to an acidic group is documented in thermodynamic and crystallographic studies (*45, 46*). Most importantly, *glycerol itself* has been observed to coordinate free Mn(II) in aqueous solution, through NMR relaxation studies (*47*). These studies set ample precedent for the coordination of glycerol by Mn(II) in p21. Both the amplitude of the deuterium signal and its saturation behavior are thus best explained by direct coordination of the Mn(II) ion by glycerol. Inasmuch as ESEEM and EPR studies in aqueous-glycerol solutions implicate the coordination of two protein and phosphate oxygen atoms in p21 · Mn(II)GMPPNP, glycerol must be replacing aquo ligands of the Mn(II).

In light of the widespread use of glycerol as a cryoprotectant (*25, 26*), these results underscore the general importance of probing the effects of glycerol on the structure and function of the system under study. In the particular case of p21, we are especially interested in the interactions between the Mn(II) and the nucleotide and protein. Such interactions could conceivably be disrupted if active site water molecules are replaced by glycerol.

The behavior of MG, as contrasted with glycerol, likely stems from the fact that MG is a bulkier molecule with a ring structure that hinders its access to the active site cation, whereas glycerol is a relatively small, open-chain molecule. If the deuterium ESEEM from d_7-MG arises from a *single* molecule bound near the active site, it is located at a distance ~1.5 times greater than the glycerol ligand—a distance difficult to reconcile with coordination to the Mn(II) ion. Moreover, this remoteness, together with the comparative bulkiness of MG, suggests that some caution should be exercised in assuming that ESEEM is dominated by the single nearest molecule to the Mn(II) ion.

[3] The deuterium modulation amplitudes cannot be accounted for by contributions from more distant molecules that are also more numerous—e.g., glycerol molecules in the second coordination sphere of the metal ion, or at even more remote locations. In order to account for the amplitude of the modulations by second sphere coordination, six glycerol molecules would have to surround the Mn(II) ion at a distance of ~5.5 Å. Our previous ESEEM studies of p21 have shown direct coordination of the polyphosphate chain of GMPPNP as well as Ser 17 (*1*). EPR studies with $H_2{}^{17}O$ have shown that only two water molecules coordinate the divalent metal ion, implying that the metal ion is predominantly surrounded by protein (*2*). Consistent with this observation is the fact that X-ray studies have indicated that there are four ligands to the divalent ion belonging to the protein or the tightly bound GMPPNP and two waters which complete the octahedral coordination scheme (*3*). Further, the structure of p21 indicates that the metal ion is essentially sequestered from bulk solvent (see below) and only three water molecules appear to be in the second sphere (*2*). Indeed, the fact that the metal ion is nearly surrounded by protein and nucleotide makes it very unlikely that six glycerol molecules could fit into the second coordination sphere of Mn(II). Successively more distant solvation spheres cannot account for the observed amplitude, owing to the much more rapid decrease of modulation depth, which declines as r^{-6}, than the increase in the number of solvent molecules, which can rise only as r^2.

Cryoprotectant deuteration was found to provide a small increase in T_m for samples prepared with glycerol but not MG. This observation reinforces the results of the ESEEM measurements regarding the relative distances between the Mn(II) ion and the hypothetically closest cryoprotectant molecules. A glycerol molecule must be in close proximity to the Mn ion so that spin flip-flop processes of glycerol hydrogen nuclei are effective in generating fluctuating fields at the Mn(II) ion and hence a shorter T_m value is obtained. Deuterium, with a gyromagnetic ratio 6.5 times smaller than that of hydrogen, generates significantly smaller fields and does not affect T_m. The proton spin flip-flop processes are allowed so long as they are energy conserving, a condition satisfied when the glycerol proton hyperfine splittings are smaller than the matrix proton linewidth (~100 KHz). From simulation of the deuterium peak amplitudes of the deuterated glycerol samples, we estimate proton hyperfine couplings of 0.1–0.4 MHz; this range of couplings indicates that some protons of the coordinated glycerol molecule are not detuned from the matrix protons and energy conserving flip-flop processes may occur. In contrast, the local field exerted at the Mn(II) ion by hyperfine interactions with the MG hydrogen nuclei is not effective in shortening T_m, suggesting that MG is more distant from the active site than glycerol.

Distances between Mn(II) and selectively labeled protein nuclei. Our previous ESEEM results provided measurements to selected nuclei on p21 that were generally in agreement with those derived from X-ray crystallography (*1, 35*). The distances we observed between Mn(II) and several nuclei on Thr35 in the GTP form of p21, however, place this critical residue (*34*) farther from the metal than observed in the crystal structure. We concluded that the interaction between the hydroxyl group and the Mn(II) ion must be relatively weak in solution (*1, 36*). We suggest that intermolecular (protein–protein) forces probably alter the interaction between Thr35 and the metal in the crystal or that these crystal contacts reduce the mobility of loop 2 observed in solution (*35*). This situation is precedented by the differences in the coordination of zinc exhibited in Concanavalin A in solution vs in crystals (*21*) and in the coordination of zinc and cobalt in carboxypeptidase A (*48*).

The coordination of the hydroxyl group of Thr35 to the active site cation has been described as the driving force for inducing the conformational change that is critical to signal transduction in p21 (*34*). Accordingly, the discrepancy between the crystal and solution structures deserves close scrutiny. In particular, the possibility that the ESEEM distance measurements are artifactually influenced by the sample freezing process or by the presence of cryoprotectant additives must be examined. Moreover, since we have established (*vide supra*) that glycerol replaces water molecules at the active site of p21, it is important to determine whether this substitution has significant structural or functional consequences.

Detailed analyses of the ESEEM results presented in Figs. 3 and 4 indicate that the distances between the Mn(II) ion and the

observed nuclei, including nuclei on Thr 35, are unaffected by either the presence or the varied concentration of glycerol or MG. Therefore, the presence of glycerol or MG cannot be the cause of the differences between the ESEEM and X-ray structural results. Moreover, the distances for these nuclei are also the same in a sample that was spray-frozen in the presence of 5% MG. Since spray-freezing takes place in only a few milliseconds, the protein can sample only the conformations available to it on this time scale; therefore, the possibilities for conformational re-equilibration are severely circumscribed (*28*). These results confirm that the distance between the Mn(II) ion and the Thr35 deuterium label in [^{2}H-3]Thr-labeled p21·GMPPNP, in frozen aqueous solution, is 4.9 ± 0.2 Å, independent of the presence of cryoprotectant additives or the sample cooling rate, and indicate that the greater Mn(II)-^{2}H distance observed in frozen solution versus the crystalline state is not ordained by the freezing method. As viewed in solution, therefore, the coordination of the Thr35 hydroxyl to the Mn(II) must involve an unusually long Mn(II)-oxygen bond. As we have previously argued on the basis of ESEEM and EPR measurements, and on strictly energetic grounds, the metal coordination of the Thr35 hydroxyl group cannot drive, but evidently simply accompanies, the biologically crucial conformational change induced by the replacement of GDP by GTP in p21 (*1, 36*).

GTPase activity. As a further check on the influence of cryoprotectants, we assayed the GAP334-accelerated hydrolysis of p21-bound GTP in solutions containing glycerol, MG, and sucrose. GAP334 may be considered to be an enzyme, with p21GTP its substrate and p21GDP+Pi the products of its catalytic reaction. Let k_1 be the rate constant for the association of GAP334 and p21GTP, k_{-1} be the dissociation rate constant, and k_2 be the rate constant for conversion to products (Scheme 1). In this mechanism the Michaelis constant, K_m, = $(k_2 + k_{-1})/k_2$ and $k_{cat} = k_2$ (*49*). We assayed the GAP334-dependent GTPase activity with [p21GTP] = 1 μM—a concentration much smaller than its Michaelis constant, 19 μM (*38*). Under these circumstances, the ratio of the reaction rate coefficient to the enzyme concentration is k_{cat}/K_m. We found the activity in the presence of as much as 15% sucrose, 15% MG, or 50% glycerol to be at least ~70% of the velocity in the absence of these substances (Tables 2 and 3), thus maintaining a $\sim 10^4$ enhancement of the basal (GAP334-independent) GTPase rate. These results imply that sucrose, MG, and glycerol do not significantly alter the ability of GAP334 to recognize p21GTP or the ability of the GAP334·p21GTP complex to react. In addition, the rate of reaction is slightly faster in the presence of Mn(II) than in the presence of Mg(II). This strongly argues that Mn(II) is a conservative replacement for Mg(II) the putative cofactor *in vivo.*

The data also indicate that GAP334-dependent GTP hydrolysis operates under equilibrium, rather than under diffusion-controlled conditions. The addition of cryoprotectants increases the viscosity of the solution, which may reduce the rate

$$\text{GAP334+p21GTP} \underset{k_{-1}}{\overset{k_1}{\rightleftharpoons}} \text{GAP334•p21GTP} \xrightarrow{k_2} \text{GAP334+p21GDP}$$

SCHEME 1

of reaction (*50–52*). If $k_2 \gg k_{-1}$, then $k_{cat}/K_m = k_1$, and this quotient should vary inversely with solvent viscosity; in this regime, the reaction operates under diffusion-control. If, however, $k_2 \ll k_{-1}$, then $k_{cat}/K_m = k_2/K_s$ and the viscosity effects on k_1 and k_{-1} cancel; in this regime, the reaction operates under essentially equilibrium conditions, with $K_m = K_s = k_{-1}/k_1$ (*52*). The extensive results with glycerol, over the viscosity range 0.9 to 5.2 p (Table 3), evince little variation in k_{cat}/k_m; similar results were found in more limited studies with sucrose and MG (Table 2). These results indicate that the GAP334·p21GTP complex dissociates more quickly than it forms products, i.e., that $k_{-1} \gg k_2$, and thus GAP334 operates under equilibrium conditions. The dissociation constant, K_s, of the GAP334·p21GMPPNP complex to GAP334 and p21GMPPNP is 21 μM (*38*). This value is essentially equal to the value of K_m, 19 μM, for the GAP334 catalyzed hydrolysis of p21GTP (*38*). If one assumes that the dissociation constant for GAP334·p21GMPPNP is equal to the value for GAP334·p21GTP, the similarity of K_s to K_m for GAP334·p21GTP supports our conclusion that GAP334 functions under equilibrium, rather than diffusion-controlled conditions.

The ESEEM results presented here, together with related ESEEM studies of model complexes (Luchsinger *et al.*, unpublished results) and high-field EPR measurements (*2*) indicate that, at the concentrations of glycerol normally employed for cryoprotection, the two aquo ligands of the Mn(II) in p21·GMPPNP are replaced by a glycerol molecule. The absence of a significant effect on the GAP334-accelerated GTPase rate, despite the replacement of these aquo ligands, supports the conjecture (*3*) that the active nucleophile in the hydrolysis reaction derives from a water molecule that is *not* coordinated to the metal ion. In this regard the behavior of the GAP334·p21GTP complex differs from, for example, staphylococcal nuclease (*6*), but is analogous to ribonuclease H, which retains essentially full activity when its Mg(II) ion is replaced by $Co(NH_3)_6^{3+}$, and which therefore cannot require a metal-coordinated water molecule in its catalytic reaction (*53*). In an interesting further parallel, when the amine ligands in the cobalt complex are replaced by bulkier ethylenediammine ligands—akin to a glycerol for water substitution—the activity of ribonuclease H remains essentially unaffected.

Cryoprotectant–protein interactions. Despite the numerous advantages that accompany their use, cryoprotectants inevitably introduce the potential for interactions that perturb the molecule under investigation. At one extreme is the potential for covalent modification. For example, certain sugars, including glucose, can glycosylate a protein by Schiff base formation with its lysine residues (*54*). This problem is easily avoided, of course, since glycerol as well as glycosides like sucrose and

MG do not react in this fashion. Weak interactions at the protein-solvent interface might lead to more subtle effects. In mixtures of water and glycerol, however, proteins tend to be preferentially hydrated (*55*). Methods such as fluorescence emission and circular dichroism have proven useful in probing for structural perturbations induced by such weak interactions (*20, 50*).

The replacement of water inside a protein, at its active site, exemplifies an intermediate case. Polyhydroxylic compounds have been observed to act as alternate acceptors (substrates) in place of water in acyl- and phosphoryl-group transfer reactions (*19, 52*). These observations suggest that the polyhydroxylic compounds bind at the active sites of these enzymes in place of water, but do so without significantly changing the protein structures, inasmuch as the enzyme function is maintained. Enzymatic properties of a number of proteins more closely related to p21—members of the G-protein superfamily—have also been studied in glycerol-containing solutions. Our conclusion that glycerol can bind to the metal cation in the p21 suggests that glycerol–metal interactions might also be important in these related proteins, and be involved in some of the intriguing effects that glycerol has on their actions. For example, in the case of the elongation factor EF-Tu, glycerol concentrations greater than 10% inhibit the GTPase of the wild type protein, but stabilize the GTPase rate of the D80N mutant. We note that Asp80 indirectly coordinates the divalent metal in EF-Tu through an aquo ligand bridge (*18*). The GTPase rate of tubulin is stimulated about 5-fold by 3.4 M glycerol (*15*). The binding, dissociation, and hydrolysis of guanine nucleotides to a protein complex formed from the domains of G_α were also performed in the presence of 30% glycerol (*56*). The potential for interactions that could significantly alter the enzyme kinetics emphasizes the importance of appropriate controls: either the elimination of additives or the use of nonhydroxylic compounds (*12–14*).

SUMMARY

In p21 the Mn(II)·nucleotide binding site is solvent-accessible, and therefore is also accessible to cryoprotectants, whose effect on structure and function had not been assessed. Our results show that glycerol binds in the first coordination sphere of the protein's divalent metal ion. The fact that no changes in distances between the metal ion and various nuclei within the protein are observed when we change the concentration of glycerol, use other cryoprotectants, or omit any cryoprotection implies that glycerol replaces waters of hydration. None of the cryoprotectants used had a profound effect on the GAP334-dependent GTPase rate, confirming our conclusion that the cryoprotectant is not perturbing the structure. We found that MG is equally effective per unit molarity as the more-widely used glycerol in cryoprotection, but does not coordinate directly to the metal site.

When selecting a cryoprotectant for low-temperature studies of proteins, the following criteria may be used. If the protein retains activity in the presence of the cryoprotectant, it is likely that no structural changes or chemical modifications of consequence have occurred. Because most cryoprotectants increase viscosity, it may be preferable to use alternate, slow substrates since the rate of enzymatic reactions of alternate substrates will be less affected by changes in viscosity (*50–52*). ESEEM spectroscopy in the presence of labeled cryoprotectant may be used to show the proximity of the cryoprotectant to a paramagnetic center. Other techniques include circular dichroism (*50*) and fluorescence emission (*20*) which might be sensitive to putative conformational changes brought about by the cryoprotectant. If these studies suggest that a high concentration of cryoprotectant is deleterious, the sample may be spray-frozen in the presence of a low concentration of cryoprotectant. Spray-freezing also minimizes the possibility of conformational rearrangement during cooling (*28*). Among polyhydroxylic compounds, MG and sucrose are less reactive than glucose (*54*) and are larger than glycerol, making them excellent choices. Polymeric cryoprotectants such as polvinylpyrrolidone, poly(ethyleneglycol) (*13*), and crosslinked dextran (*12, 41*) have not received as much attention as they might merit. Two cryoprotectants may be used to increase the confidence that the cryoprotectant is having no significant effect on the protein (*52*).

EXPERIMENTAL METHODS

The expression and purification of *ras* p21, the incorporation of the GTP analog, GMPPNP, and the substitution of Mn^{2+} for Mg^{2+} and the preparation of samples for spin-echo spectroscopy were carried out as described previously (*1*). The mixed aqueous solvent compositions are given by *volume* fraction for glycerol and *weight* fraction for MG and sucrose.

Synthesis of (1,2,3,4,5,6,6-d_7)methyl α-D-glucopyranoside. This compound was synthesized from 1.5 g (1,2,3,4,5,6,6-d_7) D-glucose (Cambridge Isotope Laboratories) according to a published procedure with minor modifications (*57*). HPLC grade methanol (Fisher) was dried and distilled from magnesium methoxide (*58*). The methyl α-D-glucopyranoside (MG) was recrystallized from ethanol and dried under vacuum (M.P. 165–166°C, uncorrected). Unlabeled MG (15 g, Fluka) was recrystallized from 75 mL methanol (*58*) and dried under a vacuum (M.P. 167–168°C, uncorrected).

GTPase assay. The GTPase activity of p21 catalyzed by the C-terminal portion of the GTPase activating protein (GAP334) was assayed under similar conditions to those reported previously (*38*). Buffers were adjusted to the desired pH at 24°C and made as 10-fold concentrated solutions. GAP334 was diluted into 20 mM N-(2-hydroxyethyl)-N-2-piperazine-ethanesulfonic acid (HEPES)·NaOH pH 7.5, 5 mM dithiothreitol (DTT), 1 μM each pepstatin and leupeptin, in 10% glycerol. Typically, guanosine 5′-diphosphate (GDP), was exchanged for 0.5 Ci/mmol [^{32}P]GTP (ICN) by incubating 10 μM p21 with 100 μM [^{32}P]GTP for at least 30 minutes at 25°C

in buffer A: 20 mM HEPES · NaOH (pH 7.5), 10 mM DTT, 5 mM ethylenediaminetetraacetic acid (EDTA). The total volume of the exchange mixture was 1000 μL. A PD-10 column (Pharmacia) was equilibrated in buffer B: 20 mM HEPES · NaOH (pH 7), 10 mM DTT, 0.02% sodium azide. The protein was separated from the exchange mixture using this column with buffer B as the eluent, and the protein-containing fraction was stored on ice.

Reaction mixtures of 200 μL final volume were prepared in Buffer B plus 1 mM $MgCl_2$. These consisted of 50–100 μL of p21 · GTP, 10 μL 20 mM $MgCl_2$, 20 μL Buffer B (at 10-fold concentration), 70–120 μL H_2O. In reactions run in the presence of glycerol or sucrose, these polyhydroxylic compounds replaced some or all of the volume of water. The reaction was initiated by the addition of 75 ng GAP334, and six 20-μL-aliquots were taken at 1 minute intervals. The temperature was 25°C. Inorganic phosphate (P_i) was extracted and $^{32}P_i$ counted essentially as described (*59*). Control experiments also showed that the presence of 50% glycerol had little effect on counting efficiency. We observed GAP334 to have a specific activity of 250 U/mg, similar to the previously reported value of 330 U/mg (*38*).

Freezing methodology. Two different freezing methods were assessed: plunge-freezing and spray-freezing (*32*). The majority of samples of p21 were placed in 4 mm O.D., 3 mm I.D. fused silica EPR tubes and cooled by plunging into various cryogens—including boiling nitrogen, boiling ethane, and isopentane slush—situated within an outer bath of liquid N_2. Some samples were spray-frozen by injecting tiny droplets into cold isopentane. The frozen droplets were then collected by filtration. The isopentane was removed from these samples by evacuation at approximately −77°C, and the frozen droplets were gently tamped to the bottom of the fused silica EPR tubes.

Electron spin-echo spectroscopy. Time domain ESEEM patterns were obtained at ~4.2 K, employing a spectrometer described previously (*60*). Two- and three-pulse ESEEM experiments were performed at excitation frequencies in the range of 8–12 GHz using different three-loop, two-gap resonators. Typically the ESEEM spectra were acquired with microwave excitation at an intensity maximum in the Mn(II) EPR spectrum. The two- and three-pulse echo decay envelopes were obtained by averaging 5–10 scans of 256 points/scan with a 15–30 ns step size. The echoes were repeated at a rate of ~500 Hz.

The peak amplitudes of weakly coupled nuclei in ESEEM spectra of p21 · Mn(II)nucleotide indicate the strength of the electron–nuclear dipolar interaction, and thus, the distance between the (S=5/2) Mn(II) ion and the coupled nucleus is obtained (*1*). The method of spectral analysis used to obtain the peak amplitudes for the observed, weakly coupled deuterium nuclei is the same as that discussed extensively elsewhere (*61*). Briefly, the time domain patterns were normalized and fitted with an appropriate decay function. The decay function was subtracted from the data, which were then tapered with an extended cosine-bell function to mitigate dead time artifacts, and zero-filled to 512 data points. A Fourier transform was then applied in magnitude mode to eliminate interference effects of peaks and side-lobes found in cosine transforms as discussed previously (*1*). In ESEEM spectra of weakly coupled nuclei (*62*), the peak amplitudes scale as ν_n^{-2} where ν_n is the nuclear Zeeman frequency. Inasmuch as the various spectra were not acquired at precisely the same value of ν_n, peak amplitudes were normalized, by scaling the observed amplitudes in proportion to ν_n^{-2}.

Deuterium ESEEM amplitudes from deuterated cryoprotectants were fitted to the saturation equation

$$y = \frac{Ax}{B + x}, \qquad [1]$$

in which x is the concentration of cryoprotectant, y is the corrected deuterium peak amplitude, and A and B describe the deuterium amplitude at saturation and the dissociation constant of the cryoprotectant, respectively (*63*).

In quantifying the proximity of the different cryoprotectants, d_5-glycerol and d_7-MG, to Mn(II) from the deuterium peak intensities, we account for the number of isotopic labels—five for glycerol and seven for MG—by employing the *single nucleus approximation* and the *equivalent nuclei approximation* (*1*), which respectively give the lower and upper bounds on the distance between the Mn(II) and the nearest cryoprotectant molecule. In the single nucleus approximation, we assume that a single closest deuterium nucleus dominates the signal amplitude due to the severe distance-dependence of ESEEM amplitudes (r^{-6}, for weakly coupled nuclei). In the equivalent nuclei approximation, we assume that all of the n deuterium nuclei on the relevant molecule lie at the same distance from the paramagnetic center and therefore contribute equally to the signal amplitude. In this situation, the effective Mn-cryoprotectant distance is $n^{1/6}$ times greater than the distance that would be obtained with the single nucleus approximation. Simulations of the experimental data to extract these distance estimates were performed as described in previous work (*1*) with one exception: the weight factor previously introduced to account for the relative abundance of the isotopic label (100% in this case) is presently used to account for the fraction of available binding sites occupied by the cryoprotectant; this ratio is determined from the deuterium ESEEM amplitude saturation curve.

ACKNOWLEDGMENTS

We thank Professor Alfred G. Redfield for many helpful and insightful discussions. We thank Professor N. Dennis Chasteen (University of New Hampshire), Dr. Sugun Sun, and John Grady for technical assistance with spray-freeze experiments. We thank Dr. Julie Scheffler (Hoffman LaRoche) for the gift of GAP334. We thank Dr. Frank McCormick (Onyx Pharmaceuticals), Professor Lawrence Feig (Tufts University), and their collaborators for plasmids bearing the *ras* genes. We gratefully acknowledge the support of the National Institutes of Health under Grant 5R 37 GM20168 (to A. G. Redfield). C. J. H. was supported by NIH postdoctoral fellowship CA08872. C. T. F. was supported by NIH training Grant 5 T32 GM08313-04.

REFERENCES

1. C. J. Halkides, C. T. Farrar, R. G. Larsen, A. G. Redfield, and D. J. Singel, Characterization of the active site of p21 *ras* by electron spin-echo envelope modulation spectroscopy with selective labeling, *Biochemistry* **33,** 4019–4035 (1994).
2. B. Bellew, C. J. Halkides, G. J. Gerfen, R. G. Griffin, and D. J. Singel, High frequency (139.5 GHz) electron paramagnetic resonance characterization of Mn(II)-$H_2{}^{17}O$ interactions in GDP and GTP forms of p21 *ras, Biochemistry* **35,** 12,186–12,193 (1996).
3. E. F. Pai, U. Krengel, G. Petsko, R. S. Goody, W. Kabsch, and A. Wittinghofer, Refined crystal structure of the triphosphate conformation of H-ras p21 at 1.35 Å resolution: Implications for the mechanism of GTP hydrolysis, *EMBO J.* **9,** 2351–2359 (1990).
4. A. M. Christensen and J. Schaefer, Solid-state NMR determination of intra- and intermolecular ^{31}P-^{13}C distances for shikimate 3-phosphate and [1-^{13}C]glyphosate bound to enolpyruvylshikimate-3-phosphate synthase, *Biochemistry* **32,** 2868–2873 (1993).
5. W. B. Mims and J. Peisach, Electron spin echo spectroscopy and the study of metalloproteins, *Biol. Magn. Reson.* **3,** 213–263 (1981).
6. E. H. Serpersu, J. McCracken, J. Peisach, and A. S. Mildvan, Electron spin echo modulation and nuclear relaxation studies of staphylococcal nuclease and its metal-coordinating mutants, *Biochemistry* **27,** 8034–8044 (1988).
7. N. Roos and A. J. Morgan, "Cryopreparation of Thin Biological Specimens for Electron Microscopy: Methods and Application," Oxford Univ. Press, Oxford (1990).
8. P. Bruggeller and E. Mayer, Complete vitrification in pure liquid water and dilute aqueous solutions, *Nature* **288,** 569–571 (1980).
9. A.-S. Yang and A. S. Brill, Influence of the freezing process upon fluoride binding to hemoproteins, *Biophys. J.* **59,** 1050–1063 (1991).
10. J. Dubochet, M. Adrian, J.-J. Chang, J. Lepault, and A. W. McDowall, Cryoelectron microscopy of vitrified specimens, *in* "Cryotechniques in Biological Electron Microscopy" (R. A. Steinbrecht and K. Zierold, Eds.), pp. 114–131, Springer-Verlag, Berlin (1987).
11. N. F. Albanese and N. D. Chasteen, Origin of the electron paramagnetic resonance line widths in frozen solutions of the oxovanadium (IV) ion, *J. Phys. Chem.* **82,** 910–914 (1978).
12. A. P. MacKenzie, Non-equilibrium freezing behaviour of aqueous systems, *Philos. Trans. R. Soc. London B* **278,** 167–189 (1977).
13. R. L. Sutton, Critical cooling rates to avoid ice crystallization in aqueous cryoprotectant solutions containing polymers. *J. Chem. Soc. Faraday Trans.* **87,** 3747–3751 (1991).
14. H. Skaer, Chemical cryoprotection for structural studies, *J. Micros.* **125,** 137–147 (1982).
15. K. Gekko and S. N. Timasheff, Thermodynamic and kinetic examination of protein stabilization by glycerol, *Biochemistry* **20,** 4677–4686 (1981).
16. L. Gianfreda and M. R. Scarfi, Enzyme stabilization: State of the art, *Mol. Cell. Biochem.* **100,** 97–128 (1991).
17. J. F. Carpenter and J. H. Crowe, An infrared spectroscopic study of the interactions of carbohydrates with dried proteins, *Biochemistry* **28,** 3916–3922 (1989).
18. K. Harmark, P. H. Anborgh, M. Merola, B. F. C. Clark, and A. Parmeggiani, Substitution of aspartic acid-80, a residue involved in coordination of magnesium, weakens the GTP binding and strongly enhances the GTPase of the G domain of elongation factor tu, *Biochemistry* **31,** 7367–7372 (1992).
19. A. L. Fink, Cryoenzymology: The study of enzyme mechanisms at subzero temperatures, *Acc. Chem. Res.* **10,** 233–239 (1977).
20. R. Virden, A. K. Tan, and A. L. Fink, Cryoenzymology of staphylococcal β-lactamase: Trapping a serine-70-linked acyl-enzyme, *Biochemistry* **29,** 145–153 (1990).
21. S.-L. Lin, E. A. Stern, A. J. Kalb (Gilboa), and Y. Xhang, X-ray Absrobtion fine structure investigation of the zinc transition metal binding site of concanavalin A in solution and in the crystal, *Biochemistry* **30,** 2323–2332 (1991).
22. R. F. Tilton, Jr., J. C. Dewan, and G. A. Petsko, Effects of temperature on protein structure and dynamics, *Biochemistry* **31,** 2469–2481 (1992).
23. H. Hope, Crystallography of biological macromolecules at ultra-low temperature, *Ann. Rev. Biophys. Biophys. Chem.* **19,** 107–126 (1990).
24. X. Tan, R. Poyner, G. H. Reed, and C. P. Scholes, Electron nuclear double resonance study of the Mn^{2+} environs in the oxalate-ATP complex of pyruvate kinase, *Biochemistry* **32,** 7799–7810 (1993).
25. A. L. P. Houseman, P. E. Doan, D. B. Goodin, and B. M. Hoffman, Comprehensive explanation of the anomalous EPR spectra of wild-type and mutant cytochrome c peroxidase compound ES, *Biochemistry* **32,** 4430–4443 (1993).
26. G. Lassman, R. Odenwaller, J. F. Curtis, J. A. DeGray, R. P. Mason, L. J. Marnett, and T. E. Eling, Electron spin resonance investigation of tyrosyl radicals of prostaglandin H synthase, *J. Biol. Chem.* **266,** 20,045–20,055 (1991).
27. L. Bachmann, Freeze-etching of dispersions, emulsions and macromolecular solutions of biological interest, *in* "Cryotechniques in Biological Electron Microscopy" (R. A. Steinbrecht and K. Zierold, Eds.), pp. 192–204, Springer-Verlag, Berlin (1987).
28. A. Levy, P. Kuppusamy, and J. Rifkind, Multiple heme pocket subconformations of methemoglobin associated with distal histidine interactions, *Biochemistry* **29,** 9311–9316 (1990).
29. H. Plattner and L. Bachmann, Cryofixation: A tool in biological ultrastructural research, *Int. Rev. Cytol.* **79,** 237–304 (1982).
30. J. N. S. Evans, R. J. Appleyard, and W. A. Shuttleworth, Detection of an enzyme-intermediate complex by time-resolved solid state NMR spectroscopy, *J. Am. Chem. Soc.* **115,** 1588–1590 (1993).
31. W. H. Orme-Johnson, H. Beinert, and R. L. Blakely, Cobamides and ribonucleotide reduction, *J. Biol. Chem.* **249,** 2338–2343 (1974).
32. M. C. Brenner, C. J. Murray, and J. P. Klinman, Rapid freeze- and chemical-quench studies of dopamine β-monooxygenase: Comparison of pre-steady-state and steady-state parameters, *Biochemistry* **28,** 4656–4664 (1989).
33. J. Downward, Regulatory mechanisms for *ras* proteins, *BioEssays* **14,** 177–184 (1992).
34. M. S. Marshall, The effector interactions of p21 *ras, Trends Biochem. Sci.* **18,** 250–254 (1993).
35. C. T. Farrar, C. J. Halkides, and D. J. Singel, The active-site structure of p21 ras shows weak coordination of Thr35 to the divalent metal ion in frozen solution ESEEM studies, *Structure* **5,** 1055–1066 (1997).
36. C. J. Halkides, B. F. Bellew, G. J. Gerfen, C. T. Farrar, P. H. Carter, B. Ruo, D. A. Evans, R. G. Griffin, and D. J. Singel, High frequency (139.5 GHz) electron paramagnetic resonance spectroscopy of the GTP form of p21 *ras* with selective ^{17}O labeling of threonine, *Biochemistry* **35,** 12,194–12,200 (1996).
37. M. V. Milburn, L. Tong, D. A. M., A. Brunger, Z. Yamaizumi, S. Nishimura, and S.-H. Kim, Molecular switch for signal transduction: Structural differenced between active and inactive forms of protooncogenic *ras* proteins, *Science* **247,** 939–945 (1990).
38. P. Gideon, J. John, M. Frech, A. Lautwein, R. Clark, J. E. Scheffler, and A. Wittinghofer, Mutational and kinetic analysis of the GTPase-

activating protein (GAP)-p21 interaction: The C-terminal domain of GAP is not sufficient for full catalytic activity, *Mol. Cell. Biol.* **12,** 2050–2056 (1992).

39. I. M. Brown, Electron spin-echo studies of relaxation processes in molecular solids, *in* "Time Domain Electron Spin Resonance" (K. L. and R. N. Schwartz, Eds.), pp. 195–229, Wiley, New York (1979).

40. D. W. Rodgers, Cryocrystallography, *Structure* **2,** 1135–1140 (1994).

41. J. S. Leigh, Jr., and G. H. Reed, Electron paramagnetic resonance studies in frozen aqueous solutions: Elimination of freezing artifacts, *J. Phys. Chem.* **75,** 1202–1204 (1971).

42. R. J. Appleyard and J. N. S. Evans, Solid state NMR of glycine in frozen solution, *J. Magn. Reson.* **B 102,** 245–252 (1993).

43. W. B. Mims, J. L. Davis, and J. Peisach, The exchange of hydrogen ions and of water molecules near the active site of cytochrome C, *J. Magn. Reson.* **86,** 273–292 (1990).

44. D. R. Brown and L. Kevan, Solvation of exchangeable Cu^{2+} cations by primary alcohols in montmorillonite clay studied by electron spin resonance and electron spin echo modulation spectroscopies, *J. Phys. Chem.* **92,** 1971–1974 (1988).

45. G. Liang, D. Chen, M. Bastian, and H. Sigel, Metal ion binding properties of dihydroxyacetone phosphate and glycerol 1-phosphate, *J. Am. Chem. Soc.* **114,** 7780–7785 (1992).

46. A. Karipides, Crystal structure of ((S)-Malato)tetraaquamagnesium(II) hydrate: Versatility of (S)-malate-metal ion binding, *Inorg. Chem.* **18,** 3034–3037 (1979).

47. I. Bertini, F. Briganti, Z. Xia, and C. Luchinat, Nuclear magnetic relaxation dispersion studies of hexaaquo Mn(II) ions in water-glycerol mixtures, *J. Magn. Reson.* **A 101,** 198–201 (1993).

48. K. Zhang, B. Chance, D. S. Auld, K. S. Larsen, and B. L. Vallee, X-ray absorbtion fine structure study of and active site of zinc and cobalt carboxypeptidase A in their solution and crystalline forms, *Biochemistry* **31,** 1159–1168 (1992).

49. A. Fersht, "Enzyme Structure and Mechanism," Freeman, New York (1984).

50. Y. Pocker and N. Janjic, Enzyme kinetics in solvents of increased viscosity: Dynamic aspects of carbonic anhydrase catalysis, *Biochemistry* **26,** 2597–2606 (1987).

51. S. C. Blacklow, R. T. Raines, W. A. Lim, P. D. Zamore, and J. R. Knowles, Triose phosphate insomerase is diffusion controlled, *Biochemistry* **27,** 1158–1167 (1988).

52. T. T. Simopoulos and W. P. Jencks, Alkaline phosphatase is an almost perfect enzyme, *Biochemistry* **33,** 10,375–10,380 (1994).

53. R. Jou and J. A. Cowan, Ribonuclease H activation by inert transition-metal complexes, mechanistic probes for metallocofactors: Insights on the metallobiochemistry of divalent magnesium ion, *J. Am. Chem. Soc.* **113,** 6685–6686 (1991).

54. D. Cervantes-Laurean, D. E. Minter, E. L. Jacobson, and M. K. Jacobson, Protein glycation by ADP-ribose: Studies of model conjugates, *Biochemistry* **32,** 1528–1534 (1993).

55. B. Perez-Ramirez and S. N. Timasheff, Cosolvent modulation of the tubulin-colchicine GTPase-activating conformational change: Strength of the enzymatic activity, *Biochemistry* **33,** 6262–6267 (1994).

56. D. W. Markby, R. Onrust, and H. R. Bourne, Separate GTP binding and GTPase activating domains of a G_α subunit, *Science* **262,** 1895–1901 (1993).

57. G. N. Bollenback, Methyl α-D-glucopyranoside, *Methods Carbohyd. Chem.* **2,** 326–328 (1963).

58. D. D. Perrin, W. L. F. Armarego, and D. R. Perrin, "Purification of Laboratory Chemicals," Pergamon, Oxford (1980).

59. E. Shacter, Organic extraction of P_i with isobutanol/toluene, *Anal. Biochem.* **138,** 416–420 (1984).

60. R. G. Larsen, C. J. Halkides, and D. J. Singel, A geometric representation of nuclear modulation effects: The effects of high electron spin multiplicity on the electron spin echo envelope modulation spectra of Mn^{2+} complexes of N-*ras*p21, *J. Chem. Phys.* **98,** 6704–6721 (1993).

61. R. G. Larsen, C. J. Halkides, A. G. Redfield, and D. J. Singel, Electron spin-echo envelope modulation spectroscopy of Mn^{2+} complexes of N-*ras*p21 with selective ^{15}N labeling, *J. Am. Chem. Soc.* **114,** 9608–9611 (1992).

62. W. B. Mims, Envelope modulation in spin-echo experiments, *Phys. Rev. B.* **5,** 2409–2419 (1972).

63. K. van Holde, "Physical Biochemistry," Prentice Hall, Englewood Cliffs, New Jersey (1985).